UCRL-JC-120395
PREPRINT

Phase Transitions in Ammonium Perchlorate to 26 GPA and 700 K in a Diamond Anvil Cell

M. F. Foltz
J. L. Maienschein

This paper was prepared for submittal to the
1995 APS Topical Conference
Seattle, WA
August 13–18, 1995

July 10, 1995

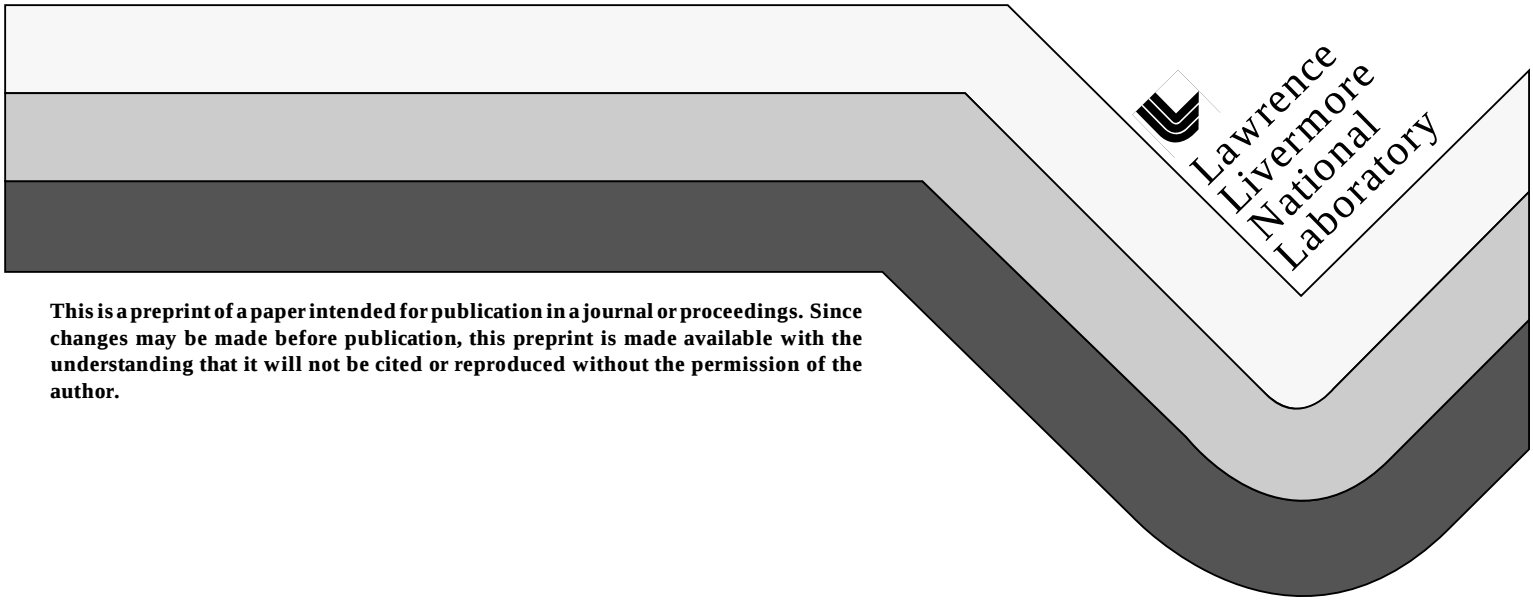

PHASE TRANSITIONS IN AMMONIUM PERCHLORATE TO 26 GPA AND 700 K IN A DIAMOND ANVIL CELL

M. Frances Foltz and Jon L. Maienschein

Lawrence Livermore National Laboratory,
P.O. Box 808, L-282, Livermore, CA 94551

Ammonium perchlorate (AP) showed previously unreported phase behavior when studied in a diamond anvil cell (DAC) at high temperature (to 693 K) and high pressure (to ~26 GPa). Liquid droplets, observed above the known 513 K orthorhombic-to-cubic phase transition, are interpreted as the onset to melting. The melting point decreased with increasing pressure. Mid-infrared FTIR spectra of the residue showed only AP. The AP melt may contribute to shock insensitivity of AP-based propellants. Gas formation was seen at higher temperatures. A phase diagram was constructed using the appearance of liquid and gas as solid-liquid and liquid-gas transitions. Preliminary pressurized differential scanning calorimetry data showed a weak pressure dependence (to ~6.9 MPa) for the orthorhombic-to-cubic phase transition.

INTRODUCTION

Ammonium perchlorate (AP; NH_4ClO_4) has long been of interest to the propellant community. In spite of extensive research (1) there is very little known about its phase diagram and the role phase transitions may play in AP reactivity and sensitivity to external stimuli. Apparent phase transitions have been noted at subambient temperatures and high pressure. (2) The reversible solid-solid transition from orthorhombic-to-cubic structure at 513 K, accompanied by a density decrease from 1.95 g/cm^3 (298 K) to 1.71 g/cm^3 (523 K), has been studied to 0.4 GPa and 573 K; in addition, an infrared analysis of AP for pressures up to 4-GPa (3) tentatively located the orthorhombic-to-cubic phase transition at 300 K and ~1.0-2.4 GPa. This phase conversion has been correlated with sudden changes in AP reactivity. No stable melt has been reported at higher temperatures, although quenched samples from pure AP and propellant combustion experiments indicate surface melting of AP may occur under pressure and temperature conditions like that in rocket motors.

We observed three apparent phase transitions over the range of 298-653 K and ambient pressure to 26 GPa, and have constructed the corresponding phase diagram. This includes phase lines corresponding to the solid-solid orthorhombic-to-cubic transition, the onset to melting, and the onset to vaporization. Gas formation was accompanied by rapid decomposition when catalyzed by metal oxide.

EXPERIMENTAL

This work, done in two stages, is described in more detail elsewhere.(1) The first set of experiments involved visual observation and video-tape recording of changes in AP pressurized in a diamond anvil cell (DAC) and heated at a constant rate to the final temperature of ~700 K. This first work provided a qualitative understanding of AP behavior. In the second set of experiments, pressure measurements were also made by the standard ruby fluorescence technique (4, 5) with chips of ruby embedded in the AP sample. Pressure calculations were based on independently measured temperature since both temperature and pressure affect the ruby R_1 line frequency shift (6, 7) Pressures were corrected for temperature effects. (1)

The ammonium perchlorate in the first work was of unknown purity; that used in the second half was as-received 99.8% pure (Aldrich). The Bassett-type DAC and pressure measurement instrumentation have been described in earlier work. (1, 8, 9) Heating ramp rates were typically ~0.17 K/s.

Relatively large (≤40-μm dia) pieces of ruby and pieces of corundum (α-Al_2O_3) were added to

some samples to test whether ruby inclusions could cause a temperature depression of observed phase transitions or act as a catalyst for AP decomposition. Al_2O_3 (ruby matrix) is not known to be catalyze AP decomposition, (10, 11) but the ruby dopant Cr_2O_3 is known to catalyze AP reactions. (11, 12)

In the second set of experiments, pressure was

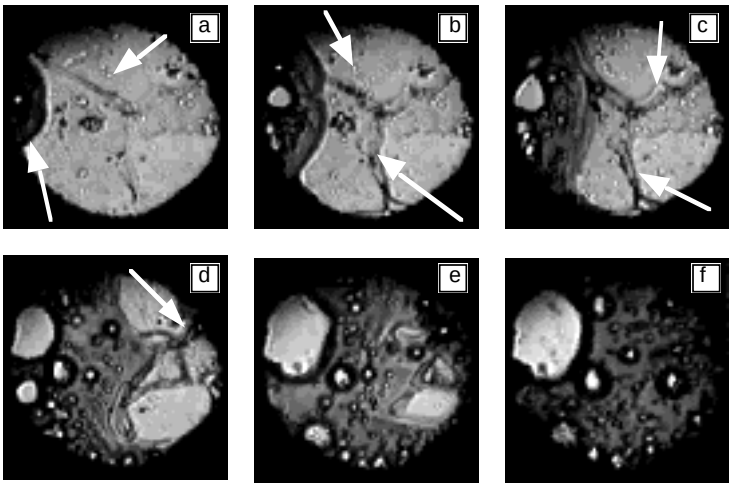

FIGURE 1. Sequence of melting, gas formation and catalyzed decomposition of AP heated at 0.17 K/s in the DAC. The initial pressure was 5.2 GPa, and the temperature ranged from 648 K (a) to 649 K (f). In (a) and (b), the upper arrow points to where we see localized melting with droplet formation. The lower arrows in (a) and (b), and the arrows in (c) and (d), point to where we see onset of bulk melting and flow of liquid. The melt/decomposition front starts at the lower arrow in (a) and sweeps left-to-right in (b) - (e). The lower arrows in (b) and (c) point to a channel where liquid from the melt/decomposition front can be seen flowing ahead of the front.

monitored (by laser-induced ruby fluorescence) as a function of the DAC body temperature. This temperature lagged 1-2 K below the gasketed sample during rapid heating (0.17 K/s), but the two temperatures agreed after 10-20 minutes of isothermal operation. The resultant temperature error of <1 % is less than the pressure error of ±5% from nonhydrostatic conditions. (13, 14)

Three experiments were done at room temperature. In two runs one of the diamonds shattered near the onset of liquid formation. Catastrophic diamond failure did not occur in the third sample, in which the AP sample was buffered from the gasket with a layer of teflon.

Continuing work involves monitoring the pressure-dependent thermal behavior of AP powder (open Pt pan, 10 K/min scan rate) in a pressurized differential scanning calorimeter module at helium pressures up to ~6.9 MPa. The sample size (~1.7-2.0 mg) is about 10^3 times larger than in the DAC.

RESULTS

Observations common to both stages of work included changes associated with the 513 K solid-solid transition, the appearance of wet spots attributed to melting, and gas formation accompanied by decomposition. Differences depended on gasket material and rate of heating used during the phase transitions. The first notable thermal behavior was the orthorhombic-to-cubic transition followed at T≥600 K. Slow heating (0.5 K/min) of AP through this transition caused the sample to fragment completely into an opaque polycrystalline powder, although this was not seen with faster heating (0.17 K/s). The next observable event at higher temperatures was the appearance of wet spots throughout the sample (Fig. 1a, 1b). For the faster heating rate, the spots increased in size and coalesced before gas formation and/or decomposition occurred at ≥620 K. For slower heating, the onset of wetting was at a higher temperature for comparable initial pressure, and gas formation and/or decomposition started at temperatures up to 675 K.

With stainless steel gaskets, rapid AP decomposition occurred simultaneously with gas bubble formation at the liquid-gasket interface. This gas-to-decomposition sequence did not start at the surface of ruby or corundum inclusions. Decomposition took the form of a sudden orange discoloration in the liquid which swept across the sample, the wake discoloring to black until the entire sample turned opaque (Fig. 1). After the DAC was cooled to room temperature, the residue in the gasket was a crusty black solid riddled with bubble marks. Due to difficult sample recovery, this material was not analyzed.

AP in inert tantalum (Ta) gaskets exhibited different behavior. Instead of discoloring to orange

and black, the wet spots coalesced to a clear liquid which was displaced by gas to nearly fill the hole. The retreat of liquid to the gasket edge left an "empty" gasket assumed to contain gas products. During cooling to room temperature, residual liquid froze to a clear solid. One Ta-confined AP sample was further heated to ~675 K after gas formation, which caused residual liquid to decompose to an opaque solid. Infrared FTIR analysis (4 cm^{-1} resolution) on room-temperature residues from samples in Ta gaskets heated only to

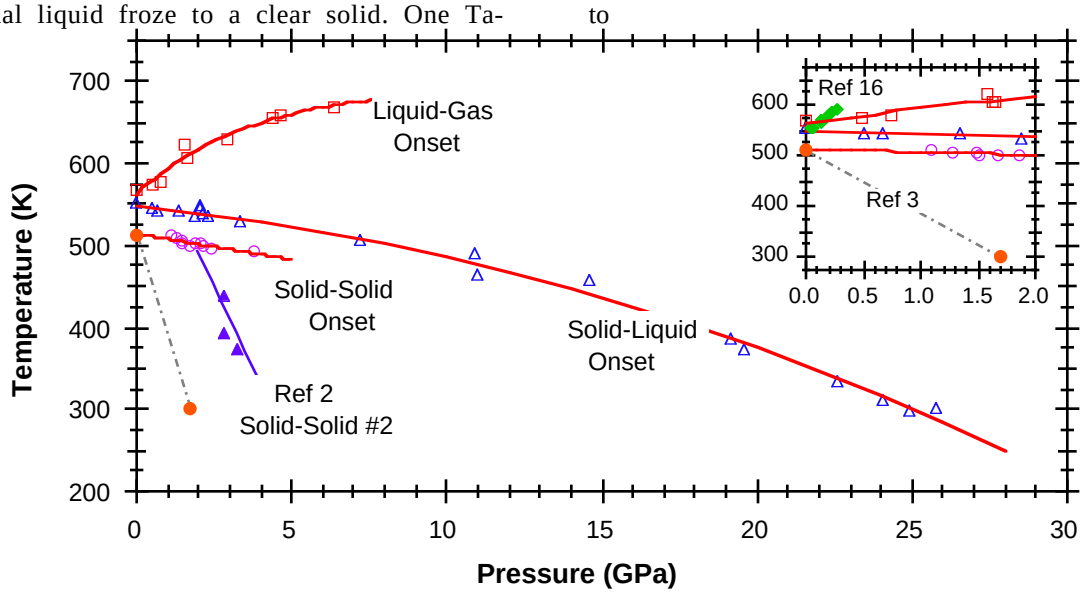

FIGURE 2. Phase diagram of ammonium perchlorate deduced from our experimental data (□, △, ○). Experimental data from Ref. 16 (◆) and 3 (●) are shown in the insert for comparison with our orthorhombic-cubic transition data(○). A second solid-solid transition (▲) from Ref. 2 is also shown. Fitted lines through the data are meant as guides for the eye and do not suggest extrapolations of data to higher pressures than measured.

melting showed AP spectral features; however, no peaks corresponding to the ClO_4^- ion (15) were seen for samples heated to vaporization, indicating at least partial decomposition.

Monitoring the onset of the orthorhombic-to-cubic transition, and solid-liquid and liquid-gas transitions, as a function of temperature and pressure allowed construction of the AP phase diagram in Fig. 2. All runs showed a drop in pressure during heating due to a thermal expansion mismatch among DAC components and sample. For samples at initial pressures <2.0-2.5 GPa, the orthorhombic-to-cubic transition was accompanied by a precipitous drop in pressure of up to 0.2 GPa - each sample had to be repressurized to continue the run. For samples at pressures of 2.5-4.0 GPa, there was a much smaller pressure drop at the orthorhombic-to-cubic transition, while at higher pressures this transition was not observed. A second isothermal pressure drop accompanied onsets to liquid and gas formation. Just beyond the liquid onset, the wet spots disappeared with the pressure drop, and then reappeared with increase in temperature. The drop in pressure between the onsets of liquid and gas formation was so extreme that to reach maximum pressure and temperature, it was necessary to repressurize the sample.

Pressurized DSC data showed no measurable difference in the onset or peak of the solid-solid endotherm up to the maximum pressure of 6.9 MPa.

DISCUSSION

The orthorhombic-to-cubic phase transition shows a weak pressure dependence of ≈ -6.3 K/GPa. This corresponds to a neglible change in melting point at the maximum PDSC pressure, in agreement with the PDSC data. The room temperature ~1.0-2.4 GPa data point of Brill, et al., (3) predicts a modest ~1 K drop in melting point at this pressure. Other experimental data using differential thermal analysis and volume displacement techniques (16) gives a positive slope of ~154 K/GPa, or a melting point elevation of +34.6 K at the maximum PDSC pressure. The lack of agreement among these studies will be discussed more elsewhere. (17)

The precipitous pressure drop seen for samples with initial pressures below 2.0-2.5 GPa is apparently a result of the stress from the orthorhombic-to-cubic transition. The product of volume expansion (13%) and bulk elasticity (3.33 P + 9.08, GPa) (1) gives the stress (P). Solving for

P shows a 2.1 GPa stress exerted by the AP on the diamonds during transition, so the diamonds were forced apart and the sample cell vented with release of pressure. At higher initial pressures, the DAC exerted enough force to contain the sample.

The solid-liquid transition shows a strong pressure dependence, and a notable downward curvature. This curvature indicates the liquid has a higher density than the solid, which is consistent with the disappearance of wet spots with drop in pressure - the formation of higher density regions pushes the entire sample to equilibrate to lower pressure. It also points to a structural instability and the possible existence of another more stable form at higher pressure.(18, 19) However, no higher pressure solid form was seen at room temperature for P≥26 GPa in this study.

The liquid-gas transition data from Ta- and stainless steel-gasketed samples were indistinguishable; thus the onset to vaporization is independent of subsequent decomposition. The rapid decomposition of AP in the 301-SS gasket is probably due to contact with the metal oxide surface film on the gasket. This observation is consistent with AP catalyzed decomposition by ferric oxide (10) and not by Al_2O_3 (10, 11) or Cr_2O_3. (11, 12)

In Ta gaskets, the AP forms a stable melt phase before decomposition sets in, which is unusual for an energetic material. The stability of the melt is consistent with an ambient pressure thermal decomposition mechanism that proceeds by proton transfer, evaporation of NH_3 and $HClO_4$, and decomposition of $HClO_{4(g)}$, the radical products of which then oxidize the NH_3. (20) Both solid-liquid and liquid-gas phase lines extrapolate at low pressure to T~550-560 K where sublimation is significant. (21) The data suggests that the process of sublimation may diverge into two reaction pathways, melting and vaporization, with the application of pressure. Since the lowest pressure measurable in the DAC was ~0.5 GPa, another pressure-dependent technique should be used to separate these processes at ambient pressure.

The existence of a solid-liquid phase transition at extreme conditions may contribute to the shock insensitivity of AP-based propellants. (22, 23) Endo-thermic melting of AP under shock will lead to a lower final temperature. Furthermore, the liquid AP can flow and fill voids, deactivating initiation sites. The exact mechanism of desensitization remains speculative, but understanding the behavior of AP-based materials under shock requires consideration of the phase transitions, particularly the solid-liquid transition reported here.

SUMMARY

The behavior of ammonium perchlorate was studied at temperatures up to 693 K and at pressures up to ~26 GPa in a diamond anvil cell (DAC). The solid-solid 513 K phase transition, and solid-liquid and liquid-gas phase lines were observed, and are shown in a proposed phase diagram of AP. Preliminary pressurized differential scanning calorimetry data agrees with a weak pressure dependence (to ~6.9 MPa) for the solid-solid phase transition. Liquid droplets interpreted as the onset to melting, were observed at temperatures above this solid transition. The melting curve plotted from this data has a downward curvature with pressure, consistent with materials for which the liquid has a higher density than the solid. At higher temperatures, gas formation followed a curve rising with increasing pressure. Due to a precipitous drop in pressure after the onset of melting, the pressure range of the measured vaporization curve was limited. Rapid decomposition took place during gas formation in the presence of metal oxide catalyst on the stainless steel gasket, but not for samples loaded in inert Ta gaskets. Mid-infrared FTIR spectra showed only AP spectral features after residue had solidified from the melt, but no ClO_4^- ion peaks in residue cooled from gas formation suggesting partial decomposition.

ACKNOWLEDGEMENTS

We thank LeRoy Green and Craig Tarver for informative technical discussions, and Jeff Davis for technical assistance with the video instrumentation. We thank W.C. Tao and the Lawrence Livermore National Laboratory Surety Program, and Louis Ullian and Loyd Parker and the Titan SRMU Impact Hazards Evaluation Program at Patrick Air Force Base, FL for financial support. This work was performed under the auspices of the U.S. Dept. of Energy by Lawrence Livermore National Laboratory under contract No. W-7405-ENG-48.

REFERENCES

1. M. F. Foltz, J. L. Maienschein, accepted for publication in *Materials Letters*, (1995); and ref. therein.
2. P. Bridgman, *Proc. Amer. Acad. Arts Sci.* **72**,45 (1937).
3. T. Brill, F. Goetz, *Laser Raman Studies of Solid Oxidizer Behavior,* T. Boggs, B. Zinns, Eds., 14th Aerospace Sciences Meeting (Amer. Inst. of Aero. and Astro., Washington, D.C., 1976), vol. 63, pp. 3-19.
4. R. Hemley, P. Bell, H. Mao, *Science* **237**, 605 (1987).
5. J. Barnett, S. Block, G. Piermarini, *Revi. Sci. Instr.* **44**, 1-9 (1973).
6. J. R. Ferraro, *Vibrational Spectroscopy at High External Pressure: The Diamond Anvil Cell* (Academic, Orlando, 1984).
7. D. M. Adams, R. Appleby, S. K. Sharma, *J. Phys. E: Sci.*

Instr. **9**, 1140-1144 (1976).
8. S. Rice, M. Foltz, *Comb. Flame* **87**, 109-122 (1991).
9. M. F. Foltz, *Prop., Expl., Pyrot.* **ech.8**, 210-216 (1993).
10. L. L. Bircumshaw, B. H. Newman, *Proc. Roy. Soc. (London)* **A227**, 115-132 (1954).
11. K. Kuratani, Aeronautical Research Institute, University of Tokyo, *Some Studies on Solid Propellants I. Kinetics of Thermal Decomposition of Ammonium Perchlorate* (1962).
12. F. Solymosi, *Combustion and Flame* **9**, 141-148 (1965).
13. H. Lorenzana, I. Silvra, K. Goettel, *Phys. Rev. Lett.* **63**, 2080 (1989).
14. G. J. Piermarini, S. Block, J. D. Barnett, *J. Appl. Phys.* **44**, 5377-5382 (1973).
15. D. J. J. Van Rensburg, C. J. H. Schutte, *J. Mol. Structure* **11**, 229-239 (1972).
16. P. Richter, C. Pistorius, *J. Solid State Chem.* **3**, 434 (1971).
17. M. Foltz, J. Maienschein, LLNL, *in prep. (1995).*
18. P. W. Bridgman, *The Physics of High Pressure* (G. Bell and Sons, London, 1958).
19. L.Liu, W. Bassett, *Elements, Oxides, and Silicates: High-Pressure Phases with Implications for the Earth's Interior* Oxford Mono. on Geol. and Geophysics (Oxford Univ. Press, New York, 1986), vol. 4.
20. A. Galwey, P. Jacobs, *J. Chem. Soc.* , 837-844 (1959).
21. P. Jacobs, H. Whitehead, *Chem Rev* **69**, 551-590 (1969).
22. P. Salzman, T. Duncan, *AIAA J.* **12**, 985-991 (1974).
23. E. James, *Propellants and Explosives in Ballistic Missiles* , UCRL-LR-113578, Lawrence Livermore National Laboratory, (July 15, 1993).

Technical Information Department • **Lawrence Livermore National Laboratory**
University of California • Livermore, California 94551